European Journal of Medicinal Chemistry 45 (2010) 4096–4103

Contents lists available at ScienceDirect

European Journal of Medicinal Chemistry

journal homepage: http://www.elsevier.com/locate/ejmech

Original article

Tricyclononene carboxamide derivatives as novel anti-HIV-1 agents

Ming-xin Dong [a], Jian Zhang [c], Xu-qing Peng [a], Hong Lu [b], Liu-hong Yun [d], Shibo Jiang [b,**], Qiu-yun Dai [a,*]

[a] Beijing Institute of Biotechnology, Beijing 100071, PR China
[b] Lindsley F. Kimball Research Institute, New York Blood Center, 310 East 67th Street, New York, NY 10065, USA
[c] Department of Pathophysiology, Key Laboratory of Cell Differentiation and Apoptosis of the Chinese Ministry of Education, Shanghai Jiao-Tong University School of Medicine (SJTU-SM), Shanghai 200025, PR China
[d] Bejing Institute of Toxicology and Pharmacology, Beijing 100850, PR China

ARTICLE INFO

Article history:
Received 26 January 2010
Received in revised form
19 May 2010
Accepted 29 May 2010
Available online 9 June 2010

Keywords:
HIV-1
Inhibitor
Synthesis
Tricyclononene carboxamide derivatives
anti-HIV-1 activity
QSAR

ABSTRACT

By modifying the chemical structure of anti-orthopoxvirus compound **ST-246**, we designed and synthesized a series of tricyclononene carboxamide derivatives and tested their anti-HIV-1 activity and cytotoxicity. We found that benzoimidazol-containing compound **7g** was highly effective in inhibiting HIV-1 R5 infection with an IC_{50} value of 0.41 μM and a selectivity index of 292, but it exhibited no significant inhibitory activity on HIV-1 reverse transcriptase, integrase and protease. CoMFA was used to analyze structure–activity relationships with good predictive power ($r^2 = 0.921$; $q^2 = 0.582$). Moreover, the CoMFA model showed that the length of the molecule, the amide, and the amine moieties all played crucial roles in anti-HIV activity. These results suggest that **7g** may serve as a lead for the development of novel anti-HIV-1 therapies.

1. Introduction

Since the 1980s, acquired immune deficiency syndrome (AIDS) has become a global epidemic disease. By the end of 2008, more than 33.2 million people had been infected worldwide, and 25 million people had died [1]. Currently, there are more than 25 drugs approved for the treatment of human immunodeficiency virus (HIV) infection. They belong to 6 classes of inhibitors and target four steps of the HIV life cycle: fusion/entry, reverse transcription, integration and proteolytic maturation [2]. The combination of reverse transcriptase inhibitors (RTIs) and protease inhibitors (PIs), commonly known as Highly Active Antiretroviral Therapy (HAART) [3], has significantly decreased morbidity and mortality among patients infected with HIV-1, transforming HIV/AIDS into a manageable chronic illness. However, HIV-1 can acquire resistance against all currently available antiviral drugs, including RTIs and PIs, the fusion inhibitor Enfuvirtide (T-20), and the CCR5 antagonist, selzentry [4–6]. Moreover, development of multidrug-resistant viruses in a growing number of patients has compromised HAART efficacy and limits therapeutic options [7]. Thus, it is still an arduous task to discover and develop new anti-HIV drugs with improved potency and resistance profiles.

Based on the chemical structure of the anti-orthopoxvirus compound **ST-246** [8], a series of tricyclononene carboxamide derivatives were designed, synthesized and evaluated for their *in vitro* antiviral activity against HIV-1 R5 strain Bal infection in CEMX174 5.25M7 cells. While a majority of these compounds moderately inhibited HIV-1 infection, the benzoimidazol-containing compound **7g** exhibited the most potent anti-HIV-1 activity with an IC_{50} (the concentration causing 50% inhibition) of 0.42 μM and a selectivity index (SI) of 292. These results suggest that compound **7g** can serve as an attractive lead for development of novel anti-HIV-1 drugs.

2. Results and discussion

2.1. Chemistry

The synthesis of the designed compounds are outlined in Schemes 1–3. The commercially available methyl 4-methylbenzoate **1** was selected as the starting material for the synthesis of compounds **7a–i**. Compound **1** reacted with NBS (1-

* Corresponding author. Tel.: +86 10 66948897; fax: +86 10 63833521.
** Corresponding author. Tel.: +1 212 570 3058; fax: +1 212 570 3099.
E-mail addresses: sjinag@nybloodcenter.org (S. Jiang), qy_dai@yahoo.com (Q.-y. Dai).

0223-5234/$ – see front matter © 2010 Elsevier Masson SAS. All rights reserved.
doi:10.1016/j.ejmech.2010.05.070

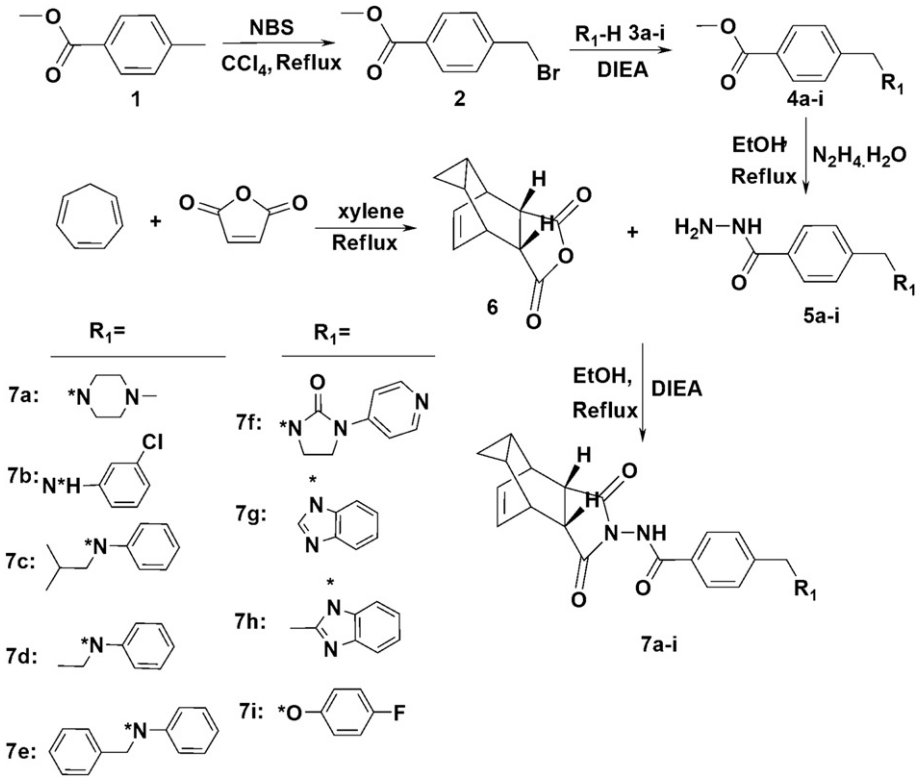

Scheme 1. Synthesis of compound **7a**–**i.**

bromopyrrolidine-2,5-dione) in refluxing tetrachloromethane to give methyl 4-(bromomethyl)benzoate **2** in 90% yield (as shown in Scheme 1). In the presence of DIEA (Diisopropyl ethylenediamine), compound **2** coupled with **3a**–**i** to provide the corresponding products **4a**–**i**. The hydrazides **5a**–**i** were prepared by treating the esters **4a**–**i** with hydrazine hydrate in refluxing ethanol for 0.5 h. The key intermediate **6** could be generated in excellent yield by treating cycloheptatriene with maleic anhydride in boiling xylene as reported in the synthesis of **ST-246** [8]. Finally, the synthesis of the target compounds **7a**–**i** were accomplished via the condensation of equimolar amounts of hydrazides **5a**–**i** and intermediate **6** in refluxing ethanol [8]. The side reaction of anhydride **6** with ethanol is suppressed because the aromatic hydrazide production is more stable than ester and water form in the condensation process as well.

For the synthesis of compounds **12a**–**i** (Scheme 2), esters **8a**, **b** and **9d**–**e** were chosen as the corresponding starting materials. Intermediates **10a** and **10c**–**e** could be prepared easily through a one-step reaction, while compound **10b** was obtained in a four-step procedure according to a known literature procedure [9,10]. Then, target compounds **12a**–**i** could be synthesized by the procedures described for the synthesis of **7a**–**i**.

As shown in Scheme 3, heating equimolar amounts of starting materials **13a**–**c** and intermediate **6** in ethanol at reflux afforded

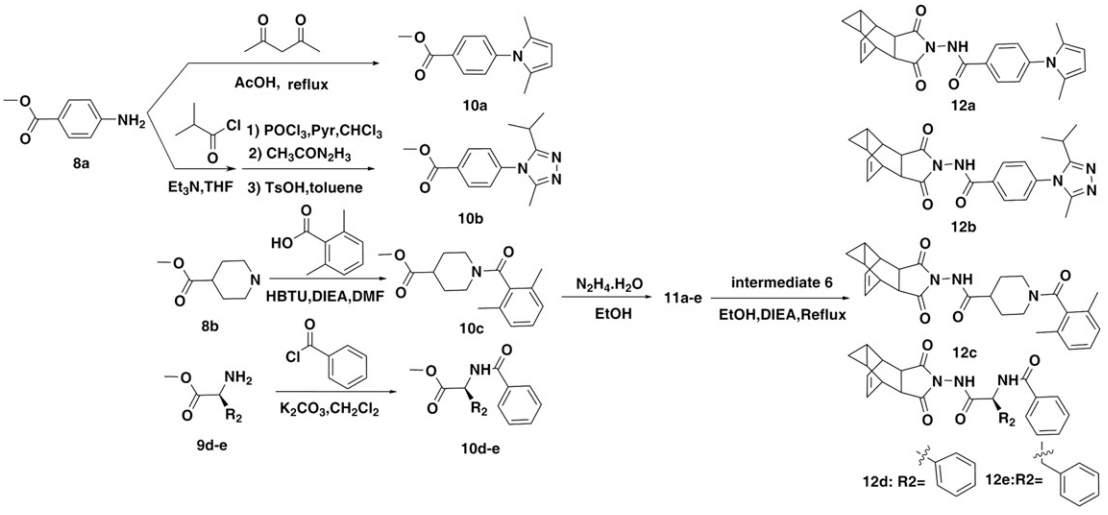

Scheme 2. Synthesis of compound **12a**–**e.**

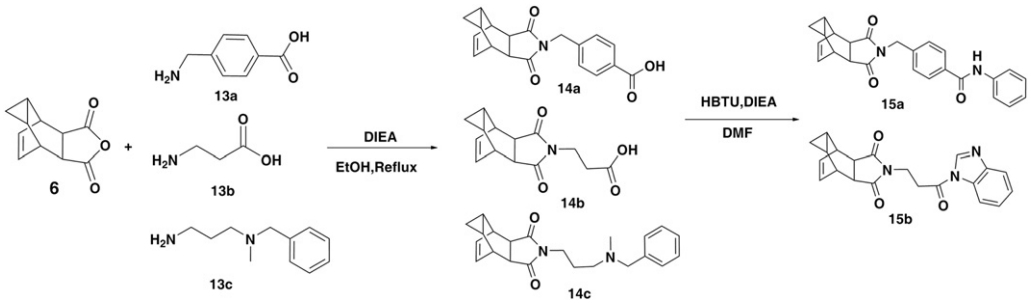

Scheme 3. Synthesis of compound **14c** and **15a**–**c**.

the target compound **14c** and intermediates **14a**, **b**. The latter coupled with the corresponding amides to obtain target compounds **15a**, **b**.

2.2. Biological evaluation

The inhibitory activities of compounds on HIV-1 R5 strain Bal infection in CEMX174 5.25M7 cells were determined by luciferase assay [11,12], and the *in vitro* cytotoxicity of compounds on CEMX174 5.25M7 cells was measured by XTT assay [13]. The IC_{50} and CC_{50} values were calculated using the CalcuSyn program [14]. The results are summarized in Table 1.

ST-246, an otherwise active compound against multiple orthopoxviruses [8,15], showed no antiviral activity against HIV-1 Bal (Table 1). However, its derivatives by replacement of the trifluoromethyl group of **ST-246**, most of which are neonatal compounds, did exhibit HIV-1 inhibitory activities. Compound **7g**, which contains benzoimidazol instead of the trifluoromethyl group of compound **ST-246**, exhibited the most potent antiviral activity (IC_{50} = 0.41 μM) and the lowest cytotoxicity (CC_{50} = 119.6 μM), values which are comparable to those of **TAK-779**, a CCR5 antagonist under development [16,17].

In contrast, compounds **7a**–**d, 7i**, **12a**, and **12b**, which contain small hydrophilic or hydrophobic groups, were much less active than compound **7g**. On the other hand, the block C (Fig. 1) should remain medium size because the compounds with bigger sized block C, such as the compounds **7e** and **7f** (Scheme 1), exhibited much lower antiviral activities (Table 1). It was unexpected that a minor change of benzoimidazol with methyl benzoimidazol (**7h**) would result in a significant increase in cytotoxicity (CC_{50} = 1.02 μM), while still maintaining antiviral activity. Taken together, block C is very sensitive to the bulk and tropism of the substitution in this region such that substituents are either too big or too small will affect its anti-HIV activity.

In addition, the soft linkers in block B might contribute to the decreased antiviral activity, such as **12c**–**e**, **14c** and **15b**. This suggests that the rigid benzamide structure is a key structural feature maintaining anti-HIV-1 activity.

Compound **7**g was also tested for inhibitory activity on HIV-1 reverse transcriptase, integrase and protease. The results showed that it exhibited no significant inhibitory activity against these enzymes at the concentration as high as 100 μM, while the corresponding inhibitors – Nevirapine, ABPS, and Indinavir, were highly effective in inhibiting the activities of reverse transcriptase, integrase and protease, respectively (Table 2). These results suggest that the compound **7g** does not target these enzymes. Since the compound **7g** exhibited potent antiviral activity against HIV-1 R5 strain (Bal), this compound may inhibit HIV-1 infection by targeting the HIV-1 coreceptor CCR5.

Table 1
Anti-HIV activities and cytotoxicities of tricyclononene carboxamide derivatives.

code	IC_{50} (μM)	CC_{50} (μM)	SI (CC_{50}/IC_{50})
ST-246	>200	ND[a]	
7a	82.81 ± 2.24	ND	
7b	13.26 ± 2.50	27.84 ± 4.87	2.01
7c	13.18 ± 1.87	32.71 ± 3.86	2.48
7d	57.21 ± 4.94	57.03 ± 13.34	1.00
7e	17.08 ± 2.16	25.49 ± 3.75	1.51
7f	>165.45	>165.45	
7g	0.41 ± 0.16	119.59 ± 5.04	291.68
7h	1.68 ± 0.38	1.02 ± 0.27	0.61
7i	31.45 ± 1.55	29.69 ± 6.17	0.94
12a	7.8 ± 0.02	3.54 ± 1.02	0.45
12b	>185.40	>185.40	
12c	>117.96	>117.96	
12d	154.8 ± 21.6	>181.20	>1.17
12e	89.40 ± 2.26	ND	
14c	30.42 ± 2.05	84.00 ± 9.79	2.76
15a	5.70 ± 1.90	44.03 ± 12.85	7.72
15b	>221.36	>221.36	
TAK-779[b]	0.05 ± 0.004	7.88 ± 0.36	157.6

[a] ND = Not done.
[b] TAK-779 is a CCR5 antagonist [16,17].

2.3. CoMFA analysis

To correlate the structure of title compound with the inhibitory activity on HIV-1 replication, a 3D QSAR analysis was performed by use of a CoMFA module following the standard procedure [18,19]. The thirteen compounds with explicit IC_{50} values were constructed by Sketch module in SYBYL. Compound **7g** was taken as a template with few rotatable bonds and high potency. CoMFA was applied to generate a predictive model, which may identify the physicochemical features of this kind of compound and provide useful information for molecular design. All compounds were fit to the common backbone for alignment, and the resultant alignments of the training set molecules are shown in Fig. 2. The IC_{50} values of the 13 structurally related compounds were subjected to CoMFA analysis. The best model was obtained with the optimum component 4, which was indicated by the cross-validation test. The cross-validation q^2 value was 0.582, and a non-cross-validated r^2 value was 0.921, with SEE (standard error of estimation) = 0.282 and F = 23.229. The contributions of steric and electrostatic fields were 59.3% and 40.7% by PLS analysis [20], respectively. This indicates that steric factors play a more important role than electronic factors on the activity of these kinds of compounds.

The predicted pIC_{50} and experimental data of the compounds are listed in Table 3. Most of the compounds were predicted correctly. Fig. 3 illustrates the contour maps of the field contributions determined by different properties as well as the template compound **7g**. The contour maps indicate how the change of the molecule affects the activity. The green contours indicate where the bulky group substitutions improve the activity, while yellow

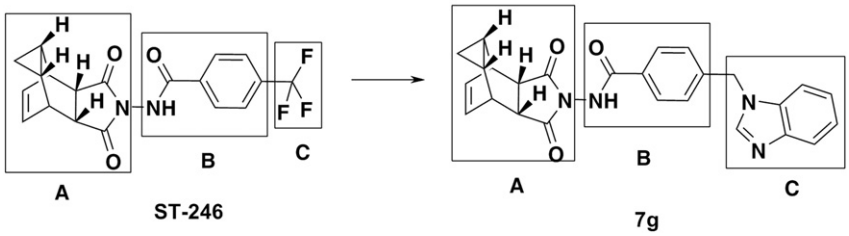

Fig. 1. The structure of ST-246 and its derivative, compound **7g**.

contours depict regions where steric bulk would not be tolerated. The blue and red polyhedrons denote the favorable sites for positively and negatively charged groups, respectively. It can be observed that most contour maps tend to focus at the right side of the molecular structures.

Since most of the diverse substitutions occurred at the right side of the compounds, the disproportion of the field distribution was generated from the limited structural changes on the left side. Within the CoMFA contour map, as shown in Fig. 3, several red polyhedrons, which indicate regions favorable to negative charge, are located on the upper middle of the molecule, nearby or pointing to the carbonyl group in the amide moiety. The amide moiety is one of the important structural characteristics of these kinds of compounds and exists in every active compound, including **TAK-799**. The red polyhedrons here show that electro-negative carbonyl oxygen has a favorable distribution for this activity. The green polyhedrons located in the lower right of the molecule indicate that the bulky group substitutions enhance the activity. The aza-indole ring indicated here gives a high potency for compound **7a**. The blue polyhedrons in the vicinity of the N atom show that the electropositive groups have an advantage with respect to affinity. However, the amine moiety is another important characteristic of these compounds and can also be found in **TAK-799**. For compounds **12d** and **12e**, the benzene ring in the right side is connected to the amide positioned near the yellow polyhedrons, but it is not long enough to extend to the green contour map region. Consequently, the activities of these kinds of compounds are relatively weak. In sum, the length of the molecule, the amide moieties and the amine moiety all play crucial roles in the affinity of the studied molecules binding to the target.

3. Conclusion

In summary, a series of tricyclononene carboxamide derivatives were synthesized and tested for their inhibitory activity against HIV-1 Bal infection in CEMX174 5.25M7 cells. Since the benzoimidazol-containing compound **7g** showed submicromolar anti-HIV-1 activity and low cytotoxicity toward the same cell line, it could act as a promising lead compound for the future optimization of CCR5 receptor inhibitor. The CoMFA model was employed to comprehensively elucidate the structure–activity relationship with good predictive power ($r^2 = 0.921$; $q^2 = 0.582$). Based on the success of this highly predictive QSAR model and CoMFA contours, further design, synthesis, biological evaluation are continuing in our laboratory.

Table 2
Inhibition of the compound **7g** on the activities of HIV-1 reverse transcriptase, intergrase and protease.

Compound	IC_{50} (μM) for inhibiting the activity of		
	Reverse transcriptase	Protease	Intergrase
Nevirapine	13.20	ND	ND
Indinavir	ND	<0.01	ND
ABPS	ND	ND	0.42
7g	>457	>114	>228

*Nevirapine, Indinavir, ABPS are inhibitors of HIV-1 reverse transcriptase, protease, and intergrase, respectively. ND = not done.

4. Experimental section

4.1. Chemistry

All chemicals and reagents used in current study were of analytical grade. Thin-layer chromatography (TLC) was performed on silica gel GF_{254} plates. Silica gel for column chromatography was obtained from Qingdao Haiyang Chemical Company. Melting points were obtained with an RY-1 melting point apparatus without correction. All ^1H NMR and ^{13}C NMR spectra were measured on a JNM-ECA-400 (400 MHz) spectrometer using tetramethylsilane (TMS) as an internal standard. Mass spectra (MS) were measured on either a Micromass ZabSpec or an ABI Perkin–Elmer Sciex API-3000 mass spectrometer with electrospray ionization.

4.1.1. The synthesis of intermediate **2**

To a stirred solution of methyl 4-methylbenzoate (3.07 g, 20 mmol) in tetrachloromethane (30 mL) was added NBS (4.14 g, 23 mmol). The mixture was heated under reflux for 5 h. After filtration, the organic layer was evaporated *in vacuo* to give 4.22 g the aimed product as yellow oil, yield: 90%.

4.1.2. General procedure for the preparation of intermediates ***4a–i***

To the solution of intermediate **2** (4.22 g, 18 mmol) in CH_2Cl_2 (35 mL) were added the corresponding starting materials **3a–i** (20 mmol) and DIEA (3.1 mL, 20 mmol), and the reaction mixture was stirred at room temperature overnight. Then, the mixture was washed with water (20 mL) and hydrochloric acid solution (2 M, 20 mL), dried (Na_2SO_4), filtered and evaporated *in vacuo* to afford the crude products **4a–i**, which were used directly in the next step without further purification.

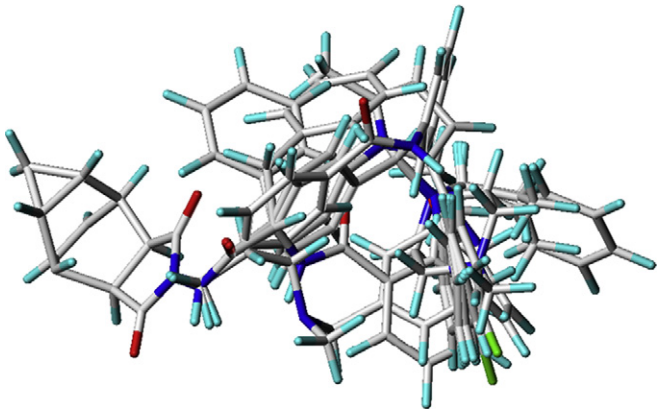

Fig. 2. Common substructure alignment.

Table 3
Experimental pIC_{50} and the corresponding predicted values for the training compounds of the CoMFA model.

Code	7a	7b	7c	7d	7e	7g	7h
pIC_{50}	4.082	4.878	4.880	4.243	4.768	6.854	5.775
Predicted pIC_{50}	4.018	4.713	4.829	4.355	4.885	6.352	6.315
Code	7i	12a	12d	12e	14c	15a	
pIC_{50}	4.502	5.108	3.810	4.049	4.517	5.244	
Predicted pIC_{50}	4.477	5.017	3.857	4.020	4.650	5.221	

*4.1.3. General procedure for the preparation of intermediates **5a–i** and **11a–e***

To the solution of intermediates **4a–i** or **10a–e** (10 mmol) in ethanol (10 mL) was added 85% hydrazine hydrate (2 mL, 30 mmol). The mixture was heated under reflux for 1 h. DM water (20 mL) was added to the reaction mixture, and the resulting product was extracted with CH_2Cl_2 (25 mL) three times. The combined organic layers were washed with DM water, dried (Na_2SO_4), filtered and evaporated *in vacuo* to give crude products **5a–i** or **11a–e**, which would be used directly in the next step without further purification.

*4.1.4. General procedure for the target compounds **7a–i**, **12a–e** and compounds **14a–c***

To a solution of intermediates **5a–i** and compound **6** (Yield: 85.4%; mp: 94–96 °C) in ethanol (5 mL) were added two drops of DIEA. The resulting mixture was heated under reflux for 6 h. Upon cooling to room temperature, the organic mixture was evaporated under reduced pressure to give a white residue. The residue was purified by column chromatography to give the target compounds **7a–i**. A similar procedure was used to synthesize **12a–e** and **14a–c**.

*4.1.4.1. N-(3,3a,4,4a,5,5a,6,6a-octahydro-1,3-dioxo-4,6-ethenocyclo-prop[f]isoindol-2 (1H)-yl)-4-(4-methylpiperazin-1-methyl)benzamide (**7a**).* White crystals, Yield 76%; mp 123–124 °C; ^{1}H NMR (400 MHz, $CDCl_3$): δ 7.79 (d, J = 8.4 Hz, 2H, Ar-H), 7.38 (d, J = 8.4 Hz, 2H, Ar-H), 5.84 (t, J = 3.6 Hz, 2H, CH=CH), 3.53 (s, 2H, Ar-CH_2), 3.46 (m, 2H, 2 × COCH), 3.14 (m, 2H, 2 × CH–CH=CH), 2.50 (m, 8H, piperazine-H), 2.34 (s, 3H, CH_3), 1.14 (d, J = 4 Hz, 2H, 2 × CH–CH_2), 0.32 (m, 2H, CH_2); ^{13}C NMR (100 MHz, DMSO-d_6): δ 174.88, 164.33, 143.28, 128.80, 127.66, 127.53, 127.24, 61.38, 54.47, 52.22, 45.36, 43.26, 42.90, 33.00, 32.71, 9.18, 4.09; MS (FAB, Glycerin) m/z calcd for $C_{24}H_{28}N_4O_3$ (M + 1): 421.2, found: 421.3.

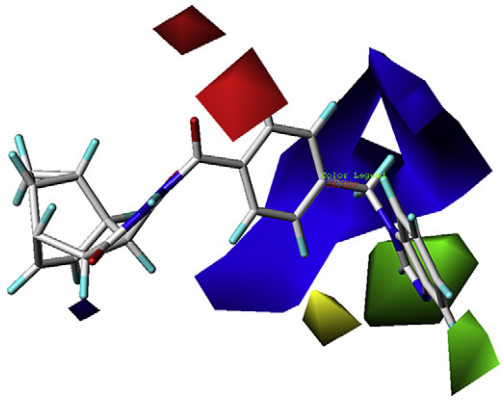

Fig. 3. Compound **7g** shown together with the contour map of CoMFA steric and electrostatic fields. Sterically favored areas (contribution level of 80%) and disfavored areas (contribution level of 20%) are represented by green polyhedron and yellow polyhedron, respectively. Blue and red polyhedrons depict the favorable site for positively (80%) and negatively (20%) charged groups, respectively.

*4.1.4.2. N-(3,3a,4,4a,5,5a,6,6a-octahydro-1,3-dioxo-4,6-ethenocyclo-prop[f]isoindol-2 (1H)-yl)-4-((3-chlorophenylamino)methyl)benzamide (**7b**).* White crystals, yield: 91%; mp: 175–177 °C; ^{1}H NMR (400 MHz, $CDCl_3$): δ 8.11(s, 1H, NH), 7.76 (d, J = 7.6 Hz, 2H, Ar-H), 7.38 (d, J = 8.4 Hz, 2H, Ar-H), 7.06 (t, J = 8.4 Hz, 1H, Ar-H), 6.70 (d, J = 8.0 Hz, 1H, Ar-H), 6.60 (s, 1H, Ar-H), 6.47 (d, J = 8.0 Hz, 1H, Ar-H), 5.83 (t, 2H, CH=CH), 4.36 (s, 2H, Ar-CH_2), 3.45 (m, 2H, 2 × COCH), 3.13 (m, 2H, 2 × CH–CH=CH), 1.13 (m, 2H, 2 × CH–CH_2), 0.32 (m, 2H, CH_2); ^{13}C NMR (100 MHz, $CDCl_3$): δ 174.86, 164.72, 148.59, 144.05, 135.05, 130.28, 129.71, 128.11, 127.80, 127.40, 117.96, 112.79, 111.31, 47.71, 43.80, 33.39, 9.59, 4.42; MS (Turbo Spray) m/z calcd for $C_{25}H_{22}ClN_3O_3$ (M + 1): 448.1, found: 448.2.

*4.1.4.3. N-(3,3a,4,4a,5,5a,6,6a-octahydro-1,3-dioxo-4,6-ethenocyclo-prop[f]isoindol-2 (1H)-yl)-4-((isobutyl(phenyl)amino)methyl)benzamide (**7c**).* White crystals, yield: 87%; mp: 158–159 °C; ^{1}H NMR (400 MHz, $CDCl_3$): δ 7.93 (s, 1H, CONH), 7.74 (d, J = 7.6 Hz, 2H, Ar-H), 7.25 (m, 2H, Ar-H), 7.17 (m, 2H, Ar-H), 6.63 (m, 3H, Ar-H), 5.83 (t, 2H, CH=CH), 4.62 (s, 2H, Ar-CH_2), 3.45 (m, 2H, 2 × COCH), 3.23 (d, J = 7.2 Hz, 2H, N–CH_2), 3.13 (m, 2H, 2 × CH–CH=CH), 2.15 (m, 1H, $CH(CH_3)_2$), 1.13 (d, J = 3.6 Hz, 2H, 2 × CH–CH_2), 0.96 (d, J = 6.8 Hz, 6H, 2 × CH_3), 0.31 (m, 2H, CH_2); ^{13}C NMR (100 MHz): δ 174.92, 164.78, 148.20, 144.52, 129.14, 128.41, 127.97, 127.76, 126.81, 116.32, 112.39, 59.91, 55.22, 43.74, 33.33, 27.34, 20.50, 9.55, 4.40; MS (Turbo Spray) m/z calcd for $C_{29}H_{31}N_3O_3$ (M + 1): 470.2, found: 469.8.

*4.1.4.4. N-(3,3a,4,4a,5,5a,6,6a-octahydro-1,3-dioxo-4,6-ethenocyclo-prop[f]isoindol-2 (1H)-yl)-4-((enthyl(phenyl)amino)methyl)benzamide (**7d**).* White crystals, yield: 90%; mp: 155–156 °C; ^{1}H NMR (400 MHz, DMSO-d_6): δ 11.03 (s, CONH), 7.83 (m, 2 H, Ar-H), 7.34 (m, 2H, Ar-H),7.10 (m, 2H, Ar-H), 6.62 (m, 3H, Ar-H), 5.79 (m, 2H, CH=CH), 4.59 (s, 2H, Ar-CH_2), 3.48 (m, 2H, CH_2CH_3), 3.28 (m, 4H, 2 × COCH, 2 × CH–CH=CH), 1.15 (m, 2H, 2 × CH–CH_2), 1.13 (m, 3H, CH_3), 0.27 (m, 2H, CH_2); ^{13}C NMR (100 MHz, $CDCl_3$): δ 175.00, 164.78, 147.98, 144.85, 129.25, 128.01, 127.72, 126.68, 116.36, 112.09, 53.79, 45.33, 43.72, 33.31, 12.09, 9.53, 4.39; MS (Turbo Spray) m/z calcd for $C_{27}H_{27}N_3O_3$ (M + 1): 442.2, found: 442.3.

*4.1.4.5. N-(3,3a,4,4a,5,5a,6,6a-octahydro-1,3-dioxo-4,6-ethenocyclo-prop[f]isoindol-2 (1H)-yl)-4-((benzyl(phenyl)amino)methyl)benzamide (**7e**).* White crystals, yield: 64%; mp: 162–163 °C; ^{1}H NMR (400 Hz, $CDCl_3$): δ 8.13 (s, 1H, CONH), 7.76 (m, 2H, Ar-H), 7.31 (m, 7H, Ar-H), 7.17 (m, 2H, Ar-H), 6.71 (m, 3H, Ar-H), 5.83 (t, 2H, CH=CH), 4.64 (d, 4H, 2 × Ar-CH_2), 3.45 (m, 2H, 2 × COCH), 3.13 (m, 2H, 2 × CH–CH=CH), 1.12 (m, 2H, 2 × CH–CH_2), 0.31 (m, 2H, CH_2); ^{13}C NMR (100 MHz, $CDCl_3$): δ 174.85, 164.76, 148.68, 144.26, 138.10, 129.29, 128.66, 128.41, 128.07, 127.80, 127.04, 126.92, 126.68, 117.20, 112.53, 54.40, 54.08, 43.76, 33.35, 9.57, 4.41; MS (Turbo Spray) m/z calcd for $C_{32}H_{29}N_3O_3$ (M + 1): 504.2, found: 504.4.

*4.1.4.6. N-(3,3a,4,4a,5,5a,6,6a-octahydro-1,3-dioxo-4,6-ethenocyclo-prop[f]isoindol-2 (1H)-yl)-4-((2-oxo-3-(pyridin-4-yl)imidazolidin-1-yl)methyl)benzamide (**7f**).* White crystals, yield: 32%; mp: >250 °C; ^{1}H NMR (400 MHz, DMSO-d_6): δ 11.08 (br, 1H, CONH), 8.40 (d, J = 5.2 Hz, 2H, pyridine-H), 7.90 (d, J = 7.6 Hz, 2H, Ar-H), 7.58 (d, J = 6.4 Hz, 2H, Ar-H), 7.46 (d, J = 8 Hz, 2H, pyridine-H), 5.80 (t, 2H, CH=CH), 4.50 (s, 2H, Ar-CH_2), 3.85 (dd, J_1 = 2.4 Hz, J_2 = 6.0 Hz, 2H, imidazolidin-CH_2), 3.44 (dd, J_1 = 8.4 Hz, J_2 = 8.0 Hz, 2H, imidazolidin-CH_2), 3.29 (m, 4H, 2 × COCH, 2 × CH–CH=CH), 1.12 (m, 2H, 2 × CH–CH_2), 0.26 (m, 2H, CH_2); ^{13}C NMR (100 MHz, CD_3OD): δ 176.90, 158.42, 149.97, 149.44, 143.03, 129.41, 129.28, 129.11, 128.92, 112.77, 112.63, 45.01, 42.76, 42.27, 39.07, 34.77, 10.44, 4.74; MS (Turbo Spray) m/z calcd for $C_{27}H_{25}N_5O_4$ (M + 1): 484.2, found: 484.3.

*4.1.4.7. N-(3,3a,4,4a,5,5a,6,6a-octahydro-1,3-dioxo-4,6-ethenocycloprop[f]isoindol-2 (1H)-yl)-4-((1H-benzo[d]imidazol-1-yl)methyl) benzamide (**7g**).* White crystals, yield 60%; mp: 272–274 °C; ^{1}H NMR (400 MHz, DMSO-d_6): δ 11.05 (s, 1H, CONH), 8.42 (s, H, imidazol-2-H), 7.85 (m, 2H, Ar-H), 7.67 (m, 1H, Ar-H), 7.42 (m, 3H, Ar-H), 7.20 (m, 2H, Ar-H), 5.78 (t, 2H, CH=CH), 5.60 (s, 2H, Ar-CH_2), 3.32(m, 4H, 2 × COCH, 2 × CH–CH=CH), 1.07 (m, 2H, 2 × CH–CH_2), 0.26 (m, 2H, CH_2); ^{13}C NMR (100 MHz, CD_3OD): δ 176.60, 144.59, 143.18, 142.19, 129.28, 128.64, 128.25, 124.50, 123.81, 111.66, 44.73, 34.47, 10.18, 4.53; MS (FAB, Glycerin) *m/z* calcd for $C_{26}H_{22}N_4O_3$ (M + 1): 439.2, found: 439.2(M + 1).

*4.1.4.8. N-(3,3a,4,4a,5,5a,6,6a-octahydro-1,3-dioxo-4,6-ethenocycloprop[f]isoindol-2 (1H)-yl)-4-((2-methyl-1H-benzo[d]imidazol-1-yl) methyl)benzamide (**7h**).* White crystals, yield: 74%; mp: 261–262 °C; ^{1}H NMR (400 MHz, $CDCl_3$): δ 10.62 (s, 1H, CONH), 7.88 (d, *J* = 8.0 Hz, 2H, Ar-H), 7.68 (d, *J* = 7.6 Hz, 1H, Ar-H), 7.23 (m, 3H, Ar-H), 6.94 (d, *J* = 7.6 Hz, 2H, Ar-H), 5.68 (t, 2H, CH=CH), 5.35(s, 2H, Ar-CH_2), 3.43 (m, 2H, 2 × COCH), 3.12 (m, 2H, 2 × CH–CH=CH), 2.35 (s, 3H, CH_3), 1.11 (d, *J* = 4.4 Hz, 2H, 2 × CH–CH_2), 0.28 (m, 2H, CH_2); ^{13}C NMR (100 MHz, CD_3OD): δ 174.82, 164.12, 151.89, 142.34, 141.65, 135.28, 130.12, 128.21, 127.52, 127.22, 126.78, 121.71, 121.42, 118.33, 109.94, 45.96, 43.26, 42.89, 32.98, 32.69, 13.57, 9.16, 4.07; MS (Turbo Spray) *m/z* calcd for $C_{27}H_{24}N_4O_3$ (M + 1): 453.2, found: 453.1.

*4.1.4.9. N-(3,3a,4,4a,5,5a,6,6a-octahydro-1,3-dioxo-4,6-ethenocycloprop[f]isoindol-2 (1H)-yl)-4-((4-fluorophenoxy)methyl)benzamide (**7i**).* White crystals, yield: 85%; mp: 189–191 °C; ^{1}H NMR (400 MHz, $CDCl_3$): δ 8.03(s, 1H, CONH), 7.83 (d, *J* = 8.4 Hz, 2H, Ar-H), 7.48 (d, *J* = 8.0 Hz, 2H, Ar-H), 6.98 (m, 2H, Ar-H), 6.89 (m, 2H, Ar-H), 5.84 (t, 2H, CH=CH), 5.07(s, 2H, Ar-CH_2), 3.46 (m, 2H, 2 × COCH), 3.14 (m, 2H, 2 × CH–CH=CH), 1.13 (m, 2H, 2 × CH–CH_2), 0.31 (m, 2H, CH_2); ^{13}C NMR (100 MHz, CD_3OD): δ 176.71, 174.19, 159.75, 157.37, 155.98, 143.62, 129.34, 128.90, 128.71, 128.25, 128.02, 116.96, 116.87, 116.66, 116.41, 70.53, 46.94, 44.79, 35.84, 34.77, 34.57, 10.23, 10.06, 4.55, 3.08; MS (Turbo Spray) *m/z* calcd for $C_{25}H_{21}FN_2O_4$ (M + 1): 433.1, found: 433.4.

*4.1.4.10. N-(3,3a,4,4a,5,5a,6,6a-octahydro-1,3-dioxo-4,6-ethanocycloprop[f]isoindol-2 (1H)-yl)-4-(2,5-dimethyl-1H-pyrrol-1-yl)benzamide (**12a**).* White crystals, yield: 86%; mp: 224–226 °C; ^{1}H NMR (400 MHz, $CDCl_3$): δ 7.95 (m, 2H, Ar-H), 7.31 (m, 2H, Ar-H), 5.93 (s, 2H, pyrrole-CH=CH), 5.86 (t, *J* = 4.0 Hz, 2H, CH=CH), 3.48 (m, 2H, 2 × COCH), 3.17 (m, 2H, 2 × CH–CH=CH), 2.03 (s, 6H, 2 × CH_3), 1.16 (m, 2H, 2 × CH–CH_2), 0.34 (m, 2H, CH_2); ^{13}C NMR (100 MHz, CD_3OD): δ 176.39, 166.82, 143.95, 129.46, 129.17, 128.81, 128.45, 107.15, 44.53, 34.30, 12.64, 9.95, 4.27; MS (Turbo Spray) *m/z* calcd for $C_{24}H_{23}N_3O_3$ (M + 1): 402.2, found: 402.1.

*4.1.4.11. N-(3,3a,4,4a,5,5a,6,6a-octahydro-1,3-dioxo-4,6-ethenocycloprop[f]isoindol-2 (1H)-yl)-4-(3-isopropyl-5-methyl-4H-1,2,4-triazol-4-yl)benzamide (**12b**).* White crystals, yield: 77%; mp: 276–277 °C; ^{1}H NMR (400 MHz, $CDCl_3$): δ 8.69 (s, 1H, CONH), 8.13 (d, *J* = 8.0 Hz, 2H, Ar-H), 7.35 (d, *J* = 8.0 Hz, 2H, Ar-H), 5.86 (t, *J* = 4.0 Hz, 2H, CH=CH), 3.48 (m, 2H, 2 × COCH), 3.17 (m, 2H, 2 × CH–CH=CH), 2.78 (m, 1H, CH(CH_3)$_2$), 2.24 (s, 3H, CH_3), 1.24 (d, *J* = 6.8 Hz, 6H, 2 × CH_3), 1.17 (m, 2H, 2 × CH–CH_2),0.33 (m, 2H, CH_2); ^{13}C NMR (100 MHz, DMSO-d_6): δ 184.26, 172.99, 167.65, 159.91, 147.00, 141.58, 141.18, 138.90, 137.35, 137.06, 136.78, 69.22, 52.44, 42.50, 34.13, 30.5, 23.56, 20.09, 18.68, 13.61; MS (Turbo Spray) *m/z* calcd for $C_{24}H_{25}N_5O_3$ (M + 1): 432.2, found: 432.2.

*4.1.4.12. N-(3,3a,4,4a,5,5a,6,6a-octahydro-1,3-dioxo-4,6-ethanocycloprop[f]isoindol-2 (1H)-yl)-N-(1-(2,6-dimethylbenzoyl)piperidine-4-yl)carboxamide (**12c**).* White crystals, yield: 91%; mp: 185–187 °C; ^{1}H NMR (400 MHz, DMSO-d_6): δ 10.53 (s, 1H, CONH), 7.17 (t, *J* = 7.6 Hz, 1H, Ar-H), 7.06 (t, *J* = 6.8 Hz, 2H, Ar-H), 5.73 (t, 2H, CH=CH), 4.54 (d, *J* = 12.8 Hz, 1H, piperidine-CH), 3.24 (m, 4H, 2 × COCH, 2 × CH–CH=CH), 3.02 (m, 1H, piperidine-H), 2.89 (m, 1H, piperidine-H), 2.55 (m, 2H, piperidine-H), 2.17 (s, 3H, CH_3), 2.11 (s, 3H, CH_3), 1.86 (d, *J* = 11.6 Hz, 1H, piperidine-H), 1.68 (d, *J* = 12.8 Hz, 1H, piperidine-H), 1.50 (d, *J* = 10 Hz, 1H, piperidine-H), 1.39 (d, *J* = 8.8 Hz, 1H, piperidine-H), 1.14 (m, 2H, 2 × CH–CH_2), 0.25 (m, 2H, CH_2); ^{13}C NMR (100 MHz, CD_3OD): δ 174.74, 169.76, 135.02, 132.92, 132.79, 127.91, 126.88, 126.84, 126.61, 44.61, 42.95, 39.56, 39.44, 32.75, 28.00, 27.41, 17.32, 17.00, 8.45, 2.74; MS (Turbo Spray) *m/z* calcd for $C_{26}H_{29}N_3O_4$ (M + 1): 448.2, found: 448.1.

*4.1.4.13. N-(3,3a,4,4a,5,5a,6,6a-octahydro-1,3-dioxo-4,6-ethanocycloprop[f]isoindol-2 (1H)-yl)-N-(2-amino-2-oxo-1-phenylethyl)benzamide (**12d**).* White crystals, yield: 45%; mp: 223–225 °C; ^{1}H NMR (400 MHz, DMSO-d_6): δ11.00 (s, 1H, CONHN), 9.02 (d, *J* = 8.4 Hz, 1H, CONH), 7.94 (m, 2H, Ar-H), 7.54 (m, 3H, Ar-H), 7.45 (m, 2H, Ar-H), 7.37 (m, 3H, Ar-H), 5.95 (d, *J* = 8.0 Hz, 1H, Ar-CH), 5.72 (t, 2H, CH=CH), 3.23 (m, 4H, 2 × COCH, 2 × CH–CH=CH), 1.07 (m, 2H, 2 × CH–CH_2), 0.23 (m, 2H, CH_2); ^{13}C NMR (100 MHz, $CDCl_3$): δ 174.29, 168.74, 167.05, 136.53, 133.14, 131.90, 128.85, 128.43, 127.59, 127.25, 55.45, 43.65, 33.20, 9.46, 4.27; MS (FAB, Glycerin) *m/z* calcd for $C_{26}H_{23}N_3O_4$ (M + 1): 442.2, found: 442.2.

*4.1.4.14. N-(3,3a,4,4a,5,5a,6,6a-octahydro-1,3-dioxo-4,6-ethanocycloprop[f]isoindol-2 (1H)-yl)-N-(1-amino-1-oxo-3-phenylpropan-2-yl)benzamide (**12e**).* White crystals, yield: 88%; mp: 108–109 °C; ^{1}H NMR (400 MHz, DMSO-d_6): δ10.82 (s, 1H, CONHN), 8.68 (d, *J* = 8.4 Hz, 1H, CONH), 7.78 (m, 2H, Ar-H), 7.45(m, 8H, Ar-H), 5.75 (t, 2H, CH=CH), 4.88 (t, *J* = 8.4 Hz, 1H, COCHN), 3.19 (m, 4H, 2 × COCH, Ar-CH_2, 2 × CH–CH=CH), 1.16 (m, 2H, 2 × CH–CH_2), 0.26 (m, 2H, CH_2); ^{13}C NMR (100 MHz, $CDCl_3$): δ 174.60, 174.37, 169.58, 168.23, 135.81, 133.18, 133.03, 129.48, 128.68, 128.60, 127.67, 127.09, 52.78, 43.67, 36.78, 36.69, 33.27, 18.40, 9.51, 4.35; MS (FAB, Glycerin) *m/z* calcd for $C_{27}H_{25}N_3O_4$ (M + 1): 456.2, found: 456.2.

*4.1.4.15. N-(3,3a,4,4a,5,5a,6,6a-octahydro-1,3-dioxo-4,6-ethanocycloprop[f]isoindol-2 (1H)-yl)-N′-benzyl-N′-methylpropane-1,3-diamine (**14c**).* Yellow oil, yield: 95%; ^{1}H NMR (400 MHz, $CDCl_3$): δ 7.31(m, 5H, Ar-H), 5.66 (t, *J* = 1.6 Hz, 2H, CH=CH), 3.45 (m, 6H, 2 × COCH, Ar-CH_2, CON–CH_2), 2.93 (m, 2H, 2 × CH–CH=CH), 2.33 (t, *J* = 7.2 Hz, 2H, CH_2N(CH_3)), 2.16 (s, 3H, CH_3), 1.67 (m, 2H, CH_2(CH_2)$_2$), 1.08 (m, 2H, 2 × CH–CH_2), 0.27 (m, 2H, CH_2); ^{13}C NMR (100 MHz, $CDCl_3$): δ 178.52, 129.06, 128.20, 127.51, 127.08, 62.11, 54.38, 45.09, 41.65, 36.46, 33.33, 25.23, 9.78, 4.65; MS (Turbo Spray) *m/z* calcd for $C_{22}H_{26}N_2O_2$ (M + 1): 351.2, found: 351.3.

*4.1.5. General procedure for the preparation of target compounds **15a–b***

To the solution of intermediate **14a** or **14b** (1 mmol) in DMF (Dimethylformamide, 10 mL) were added the corresponding amide (0.1 g, 1.1 mmol) and DIEA (0.23 mL, 1.5 mmol). The solution was chilled to 0–5 °C under an atmosphere of nitrogen. HBTU (2-(1H-Benzotriazole-1-yl)-1,1,3,3-tetramethyluronium hexafluorophosphate, 0.57 g, 1.5 mmol) was added and the solution stirred for 10 min, then warmed to room temperature and stirred an additional 2.5 h. Water (50 mL) was added to the reaction mixture to precipitate the crude products. The crude products were purified by column chromatography to give the target compounds **15a**, **b**.

*4.1.5.1. N-(3,3a,4,4a,5,5a,6,6-octahydro-1,3-dioxo-4,6-ethanocycloprop[f]isoindol-2 (1H)-yl)-4-(formanilide)benzyl (**15a**).* White crystals, yield: 86%; mp: 224–226 °C; ^{1}H NMR (400 MHz, $CDCl_3$): δ 8.01 (s, 1H, CONH), 7.78 (d, *J* = 8.0 Hz, 2H, Ar-H), 7.64 (d, *J* = 8.0 Hz, 2H, Ar-H), 7.36 (m, 4H, Ar-H), 7.15 (m, 1H, Ar-H), 5.62 (t, 2H, CH=CH),

4.59 (s, 2H, Ar-CH_2), 3.37 (t, J = 1.6 Hz, 2H, 2 × COCH), 2.99 (m, 2H, 2 × CH–CH=CH),1.09 (m, 2H, 2 × CH–CH_2), 0.33 (m, 2H, CH_2); ^{13}C NMR (100 MHz, $CDCl_3$): δ 178.16, 165.42, 139.43, 137.96, 134.25, 128.91, 128.54, 127.57, 127.27, 124.43, 120.27, 45.19, 41.51, 33.39, 9.374, 4.61; MS (Turbo Spray) m/z calcd for $C_{25}H_{22}N_2O_3$ (M + 1): 399.2, found: 399.2.

*4.1.5.2. N-(3,3a,4,4a,5,5a,6,6a-octahydro-1,3-dioxo-4,6-ethanocycloprop[f]isoindol-2 (1H)-yl)-2-((1H-benzo[d]imidazol -1-yl) methanone) ethyl (**15b**).* White crystals, yield: 64%; mp: 164–166 °C; ^{1}H NMR (400 MHz, $CDCl_3$): δ 8.35 (s, 1H, imidazol-H), 8.22 (m, 1H, Ar-H), 7.80 (m, 1H, Ar-H), 7.42 (m, 2H, Ar-H), 5.66 (m, 2H, CH=CH), 3.96 (t, J = 7.2 Hz, 2H, N–CH_2), 3.40 (m, 2H, 2 × COCH), 3.27 (t, J = 7.2 Hz, 2H, $COCH_2$), 3.00 (d, J = 1.6 Hz, 2H, 2 × CH–CH=CH), 1.10 (m, 2H, 2 × CH–CH_2), 0.28 (m, 1H, CH_2); ^{13}C NMR (100 MHz, DMSO-d_6): δ 177.89, 171.73, 169.06, 143.48, 143.24, 141.86, 131.15, 127.24, 125.31, 124.63, 121.71, 119.93, 115.15, 44.61, 44.55, 33.46, 33.05, 32.90, 31.64, 9.37, 4.32; MS (Turbo Spray) m/z calcd for $C_{21}H_{19}N_3O_3$ (M + 1): 362.1, found: 362.3.

4.2. Biological evaluation

4.2.1. Reagents

HIV-1 Bal strain (R5) was obtained from the NIH AIDS Research and Reference Reagent Program. Lymphoid cell line CEMx174 5.25M7, kindly provided by C. Cheng-Mayer, is stably transduced with an HIV-1 long terminal repeat (LTR)-green fluorescent protein (GFP) reporter and luciferase reporter construct. These cells, expressing CD4 and both coreceptors, CXCR4 and CCR5 [11], were maintained in RPMI 1640 medium supplemented with 10% fetal bovine serum (FBS), 1 μg of puromycin/mL, and 200 μg of G418/mL. HIV-1 intergrase was expressed in *E. coli* transformed with F185K/C280S IN1-288 recombinant plasmid as described by Jenkins TM et al. [21].

4.2.2. Determination of the inhibitory activity of the compounds against HIV-1 Bal infection in CEMx174 5.25M7 cells

The inhibitory activities of compounds on infection by HIV-1 R5 strain Bal in CEMx174 5.25M7 cells were determined as previously described [11,12]. Briefly, 50 μl of a compound at graded concentration in triplicate was incubated with an equal volume of the HIV-1 Bal at an MOI of 0.01 at 37 °C for 30 min, followed by addition of 100 μl of CEMx174 5.25M7 cells (5×10^5/mL). After incubation at 37 °C overnight, the culture medium was replaced with fresh medium without CAP. On day 3 post-infection, the cells were harvested and lysed for analysis of luciferase activity, using a luciferase assay kit (Promega, Madison, WI) and a luminometer (Ultra 386; Tecan, Durham, NC) according to the manufacturer's instructions. The percent inhibition of luciferase activity and the concentrations for 50% inhibition (IC_{50}) were calculated using a computer program, designated CalcuSyn, kindly provided by Dr. T. C. Chou (Sloan–Kettering Cancer Center, New York) [14].

4.2.3. Determination of the inhibitory activity of the compound **7g** against HIV-1 protease, integrase and reverse transcriptase

The inhibitory activity of the compound **7g** on HIV-1 protease activity was detected using a previously reported method [22] with modification. Indinavir (MW 613.8 Da), the HIV-1 protease inhibitor, was included as a control. Briefly, 1 μL of the compound **7g** at the graded concentrations or Indinavir at 10 nM was added into 200 μL reaction buffer (0.1 mol/L CH_3COONa, pH5.0, 0.9 mol/L NaCl, 1 mmol/L DTT, 1 mmol/L EDTA, and 5 μmol/L fluorescent peptide substrate from Molecular Probes) in wells of a microtiter plate. After preincubated for 20 min at 37 °C, the reaction was initiated by the addition of the purified recombinant HIV-1 protease (provided by the Institute of Medicinal Biotechnology at Chinese Academy of Medical Sciences). The increase of fluorescence was detected at 490 nm, using 355 nm excitation wavelength in BMG POLARstar Galaxy Fluorescence Plate Readers at 37 °C.

The inhibitory activity of the compound **7g** on HIV-1 integrase activity was measured using the procedure described by Guo et al. [23]. An intergrase inhibitor, achyranthes bidentata polysaccharide sulfate (ABPS, MW: 4000 Da) was included as a control. Briefly, wells of a 96 well Covalink-NH plate (NUNC) were coated with donor substrate (5′P-ACC CTT TTA GTC AGT GTG GAA AAT CTC TAG CAGT-3′; 3′-GAA AAT CAG TCA CAC CTT TTA GAG ATC GTCA-5′), followed by three washes with PBS. The reaction mixture (20 mmol/L Tris–HCl, pH7.8, 7.5 mmol/L $MgCl_2$, 20 mmol/L DTT, 0.1% NP40, and 25 mmol/L MOPS, pH7.2), the compound **7g** or ABPS at indicated concentrations of compounds and the HIV-1 intergrase were added in a final 100 μL volume, co-incubated at 37 °C for 1 h. Then the target biotin linked DNA (5′-TGA CCA AGG GCT AAT TCA CT-3′-biotin; biotin-3′-ACT GGT TCC CGA TTA AGT GA-5′) was added, followed by an incubation at 37 °C for 1 h. After washing three times with PBS contained 0.05% Tween 20, and an incubation with 1% BSA at 37 °C for 40 min, the alkaline phosphatase reaction system was used to detected the absorbance at 405 nm.

The inhibitory activity of the compound **7g** on HIV-1 reverse transcriptase inhibitor was tested as previously described [24]. Nevirapine (MW: 266.3 Da), an HIV-1 reverse transcriptase inhibitor, was used as a reference compound. Briefly, Poly A was immobilized via its 5′-terminal phosphate to Covalink-NH microtiter plates. The reaction mixture (60 μL) contained reaction buffer (50 mmol/L Tris–HCl (pH 8.3), 6 mmol/L $MgCl_2$, 100 mmol/L KCl, 5 mmol/L DTT (DL-dithiothreitol), 0.13 mg/ml BSA, 0.31 μg/mL oligo $(dT)_{15}$, 0.26 μM biotin-11-dUTP, 0.52 μM dTTP), compound **7g** or Nevirapine at grade concentrations, and 0.04 μL of the HIV-1 reverse transcriptase (Calbiochem). After incubation at 37 °C for 1 h, the plate was washed with a wash buffer (10 mmol/L Tris–HCl (pH 7.5), 0.15 mol/L NaCl, 1 mmol/L EDTA, 0.01% Tween 20). After 100 μL of 1% BSA and SA-HRPO (streptavidin-horseradish peroxidase) (Pharmacia) in wash buffer without Tween 20 were added to each well and incubated for 30 min at 37 °C, followed by three washes with wash buffer. Then, 100 μL of TMB (tetramethylbenzidine) solution at 100 ng/mL was added before an incubation for 15 min at room temperature. The reaction was stopped by addition of 50 μL 2 M H_2SO_4 and the absorbance at 450 nm was measured by EMax Precision Microplate ELISA Reader (Molecuar Devices).

The percent inhibition and IC_{50} value of the compounds for inhibiting the activities of the HIV-1 enzymes were calculated using CalcuSyn program as described above.

4.2.4. Assessment of in vitro cytotoxicity

The *in vitro* cytotoxicity of compounds on CEMx174 5.25M7 cells was measured by XTT assays as previously described [13]. Briefly, 100 μL of the test compound at graded concentration was added to equal volumes of cells (5×10^5/mL) in wells of 96-well plates. After incubation at 37 °C for 4 days, 50 μL of XTT solution (1 mg/mL) containing 0.02 μM of phenazine methosulfate (PMS) was added. After 4 h, the absorbance at 450 nm was measured with an ELISA reader. The CC_{50} (concentration for 50% cytotoxicity) values were calculated using the CalcuSyn computer program [14].

4.3. CoMFA analysis

All computational studies were performed in the molecular modeling package SYBYL8.0 on a Dell Precision 7400 workstation. Systematic conformation search was adopted to find the lowest energy of each compound. Partial atomic charges were assigned to each atom using the Gasteigere–Hückel method. All structures of compounds were optimized using a conjugate gradient minimizer

and the standard Tripos force field with a distance-dependent dielectric function. The minimization was terminated when the energy gradient convergence criterion of 0.001 kcal/mol was achieved or when the 1000-step minimization cycle limit was exceeded. The CoMFA descriptors, steric and electrostatic field energies, were calculated using the SYBYL default parameters: 2A° grid points spacing, sp3 carbon probe atom with +1 charge and a minimum σ (column filtering) of 2.0 kcal/mol, and an energy cutoff of 30.0 kcal/mol [25].

Acknowledgements

We thank Dr. Zonggen Peng from the Institute of Medicinal Biotechnology at Chinese Academy of Medical Sciences, for the tests of inhibitory activities of HIV-1 protease, reverse transcriptase and integrase. This work was supported by the China Specific Project for Developing New Drugs during the Eleventh Five-Year Plan Period (NO. 2009ZX09103-628, 2009ZX09503-015) awarded to Q.Y.D and by NIH grant AI 46221 awarded to S.J.

References

[1] UNAIDS. Geneva, Switzerland; 2008.
[2] W.C. Greene, Z. Debyser, Y. Ikeda, E.O. Freed, E. Stephens, W. Yonemoto, R. W. Buckheit, J.A. Esté, T. Cihlar, Antivir. Res. 80 (2008) 251–265.
[3] J. Cohen, Science 296 (2002) 2320–2324.
[4] Y.X. He, J.W. Cheng, H. Lu, J.J. Li, J. Hu, Z. Qi, Z.H. Liu, S.B. Jiang, Q.Y. Dai, Proc. Natl. Acad. Sci. U.S.A 105 (2008) 16332–16337.
[5] C.S. Adamson, E.O. Freed, Drug Discov. Today 13 (2008) 424–432.
[6] R. Delgado, Enferm. Infecc. Microbiol. Clin. 11 (2008) 28–33.
[7] P. Yeni, J. Hepatol. 44 (2006) 100–103.
[8] R.B. Thomas, R.R. Susan, O. Elizabeth, J.B. Christopher, C.P. Daniel, S.C. Marc, R. Gerry, T. Sanjeev, W.H. John, O.B. Robert, R.K. Earl, A.K. Kathy, D.C. Dai, G. Yang, H. Dennis, J. Robert, J. Med. Chem. 50 (2007) 1442–1444.
[9] B.C. Jordan, B.D. Clive, PCT Int. Appl (WO). Pfizer Ltd., 2007, 066201.
[10] K. Liu, H. Lu, L. Hou, Z. Qi, C. Teixeira, F. Barbault, B.T. Fan, S.W. Liu, S.B. Jiang, L. Xie, J. Med. Chem. 51 (2008) 7843–7854.
[11] H. Lu, Q. Zhao, G. Wallace, S. Liu, Y. He, R. Shattock, A.R. Neurath, S.B. Jiang, AIDS. Res. Hum. Retroviruses 22 (2006) 411–418.
[12] Y.X. He, J.W. Cheng, J.J. Li, Z. Qi, H. Lu, M.X. Dong, S.B. Jiang, Q.Y. Dai, J. Virol. 82 (2008) 6349–6355.
[13] A.K. Debnath, L. Radigan, S.B. Jiang, J. Med. Chem. 42 (1999) 3203–3209.
[14] T.C. Chou, M.P. Hayball, Calusyn: Windows Software for Dose Effect Analysis. BIOSOFT, Ferguson, MO 63125, USA, 1991.
[15] G. Yang, D.C. Pevear, M.H. Davies, M.S. Collett, T. Bailey, S. Rippen, L. Barone, C. Burns, G. Rhodes, S. Tohan, J.W. Huggins, R.O. Baker, R.L. Mark Buller, E. Touchette, K. Waller, J. Schriewer, J. Neyts, E. Declercq, K. Jones, D. Hruby, R. Jordans, J. Virol. 79 (2005) 13139–13149.
[16] M. Baba, O. Nishimura, N. Kanzaki, M. Okamoto, H. Sawada, Y. Iizawa, M. Shiraishi, Y. Aramaki, K. Okonogi, Y. Ogawa, K. Meguro, M. Fujino, Proc. Natl. Acad. Sci. U.S.A 96 (1999) 5698–5703.
[17] T. Ikemoto, A. Nishiguchi, H. Mitsudera, M. Wakimasu, K. Tomimatsu, Tetrahedron 57 (2001) 1525–1529.
[18] R.D. Cramer, D.E. Patterson, J.D. Bunce, J. Am. Chem. Soc. 110 (1988) 5959–5967.
[19] G.F. Yang, X.Q. Huang, Curr. Pharm. Des. 12 (2006) 4601–4611.
[20] T.A. Halgren, J. Am. Chem. Soc. 112 (1990) 4710–4723.
[21] D.J. Hazuda, J.C. Hastings, A.L. Wolfe, et al., Nucleic Acid Res. 22 (1994) 1121–1122.
[22] B. Dong, T. Zhang, P.Z. Tao, Chin. J. AIDS STD. 12 (2006) 402–405.
[23] Z.M. Guo, H.S. Chen, Chin. J. Exp. Clin. Virol. 16 (2002) 119–123.
[24] Y.X. Han, J.N. Li, L.X. Fu, J.D. Jiang, Chin. J. Microbiol. Immunol. 24 (2004) 748–750.
[25] P. Shah, A. Mittal, P.V. Bharatam, Eur. J. Med. Chem. 43 (2008) 2784–2791.